Activity Report

Simulation Study of the external Beam Line of the new Bern Cyclotron Laboratory

Sara Spadola

Summer Student at the
Albert Einstein Center for Fundamental Physics,
Laboratory for High Energy Physics (LHEP), University of Bern,
Sidlerstrasse 5, CH-3012 Bern, Switzerland

Supervisor: Dr. Saverio Braccini (Saverio.Braccini@lhep.unibe.ch)

June 2011

1 The Bern Cyclotron Laboratory

A new cyclotron laboratory for radioisotope production and research is currently under construction at the Inselspital, the University Hospital in Bern. Initiated by the Inselspital and the University of Bern, this project - denominated SWAN - is the result of the successful and fruitful collaboration between public institutions and private investors. The cyclotron is located in the underground floor of a complex five stories building featuring four GMP radio pharmacy production and research laboratories, offices and patient wards.

The SWAN cyclotron laboratory consist of 2 bunkers, one for IBA Cyclone 18 MeV cyclotron and one for the 6 m long beam line. The two bunkers are independent and can be accessed by two separated doors. The cyclotron floor also includes a workshop and a physics laboratory, both connected to the two bunkers by specifically conceived connection pipes.

1.1 The IBA Cyclone 18 MeV Cyclotron

The cyclotron, 'rigged' inside the building on the 17^{th} of June 201, is a IBA CYCLONE 18/18, constructed by the Belgian company Industrial Beam applications (IBA).
It is a fixed-energy cyclotron, accelerating negative ions (H^-) up to 18 MeV and the maximum current extracted is of 150 μA (in single or dual beam).
It is also possible to add a D^- ions source and accelerating them up to 9 MeV.
The CYCLONE 18/18 featuress eight independent exit ports allowing eight target stations to be

simultaneously mounted on the cyclotron and it will be equipped with 7 targets and 1 external beam line.
The CYCLONE 18/18 is designed for negative ion acceleration, which are produced at the centre of the machine by two internal cold cathode Penning Ion Gauge sources, in this case both producing Hydrogen (H^-) ions.
The extraction of the accelerated ions in the cyclotron is done by stripping of their electrons, thus changing their charge and bending in the magnetic field. This is done by passing the beam through a thin carbon foil (carbon stripper) which allows extraction of more than 99.9% of the accelerated beam.
Negative ions also allow the simultaneous production of two beams, and then, the production of two different radioisotopes at the same time or the extensive production of highly demanded radioisotope on two identical targets.

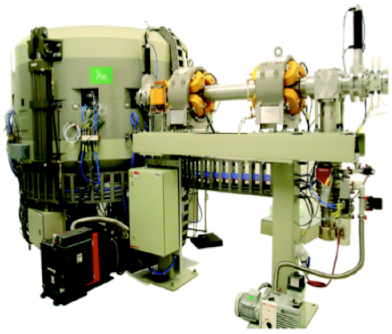

Figure 1: The IBA 18 MeV Cyclotron, equipped with a short Beam Transport Line (Courtesy IBA).

1.2 The external Beam Line

The eight exit ports located in a horizontal mid-plan all around the cyclotron give the possibility of installing an external transport beam line.
To pass from the cyclotron bunker into the research bunker, a beam-line with a length of about 6 m is needed.
The beam transport line (BTL) has the following characteristics:

1. beam line (length 6503 mm) fixed on a support;
2. a beam pipe of internal diameter of 100 mm and 110 mm of external diameter;
3. two quadrupole doublets mounted on the beam line (maximum field of 3 kG);
4. an oil diffusion pump (ODP), primary pump and vacuum valves;
5. collimators ;
6. steering magnet;

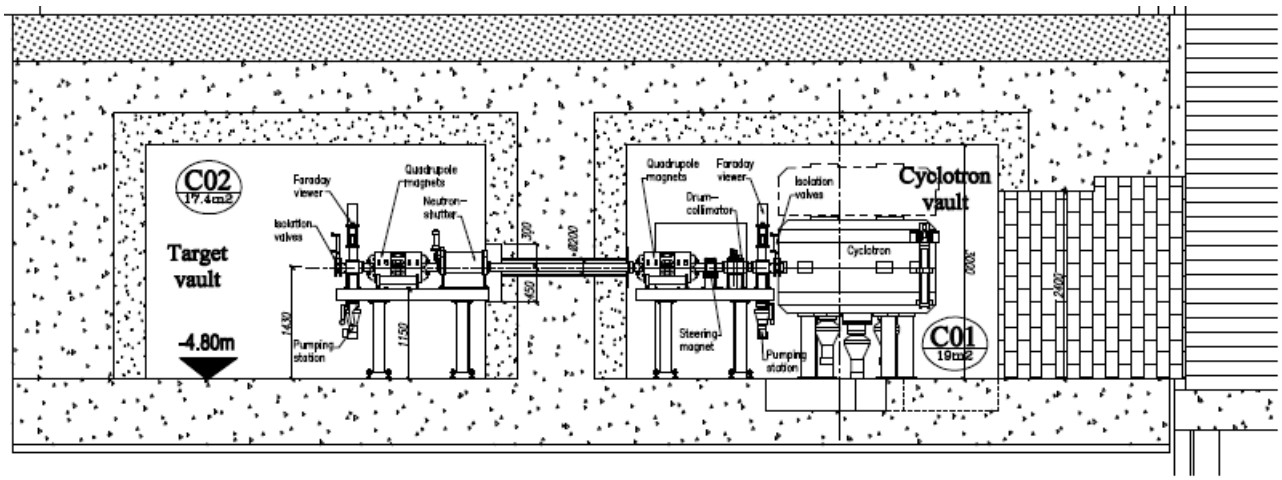

Figure 2: Scheme of the cyclotron and the external beam transport line (Courtesy IBA).

7. complete control, cooling, air-water manifold and power-supplies.

In Bern SWAN cyclotron laboratory the beam line is connected to the out port number 4. The beam line is used to transport the beam to the target vault (Fig. 2) for research purposes.

2 Design calculations

For isotope production, a beam with a beam spot of with a diameter of 10 mm or 5 mm is needed, having a waist on the target.
Provided by IBA are two settings for the quadrupoles, calculated with the TRANSPORT software from PSI for C18/18 cyclotron, BERN-SWAN project.
The quadrupole settings (pole tip field and polarity) are optimized in order to provide:

1. the beam size on target of 10 mm or 5 mm;
2. the beam at waist in both direction on the target;
3. the magnetic field which is the smallest to reduce power consumption.

The quadrupole setting to get a beam spot diameter on target of 10 mm is reported in table 1 while the one for a beam spot diameter on target of 5 mm is in table 2.

The smallest beam size that can be obtained is limited by the magnetic field that can be reached within the quadrupole (3 kG) and the beam envelope size (<35 mm); the 5 mm dimension is already close to that limit.

Table 1: Data of the quadrupole setting to get a beam spot diameter on target of 10 mm.

first doublet	H quadrupole	2,027 kG
	V quadrupole	-2,055 kG
second doublet	H quadrupole	0,976 kG
	V quadrupole	-0,464 kG

Table 2: Data of the quadrupole setting to get a beam spot diameter on target of 5 mm.

first doublet	H quadrupole	1,837 kG
	V quadrupole	-2,010 kG
second doublet	H quadrupole	2,268 kG
	V quadrupole	-2,610 kG

3 Calculations of the tunes using BeamLineSimulator

A study of the tunes using the *Beamline Simulator Software* is presented here.

3.1 The BeamlineSimulator Software

Beamline Simulator Software, by Kurt Dehnel and Morgan Dehnel, is a real-time simulator for industrial beam transport systems; it can mimic a broad range of beam transport system such as those used in radioisotope production.
The main features of the program are:

1. real time tuning capabilities;
2. the simulation of multi-particle beams of up to 10 000 particles;
3. the simulation of beam envelopes;

Beamline Simulator it's a first order modeling code ideal for quickly determining new beamline tunes.

3.2 Simulation of the beam line

The first step consist in defining the beam source with the following input data:

1. Energy = 18 MeV;
2. Mass = 938.23 MeV;
3. charge = 1q;
4. beam σ matrix (emittance) and half size.

The output beam emittance of the C18/18 in not available and, as suggested by IBA, the emittance of the C30 cyclotron was used. It should represent a good approximation.
The initial beam σ matrix is

$$\begin{pmatrix} 81 & 0.06624 & 0 & 0 & 0 \\ 0.06624 & 6.4 \cdot 10^{-5} & 0 & 0 & 0 \\ 0 & 0 & 7.29 & 0 & 0 \\ 0 & 0 & 0 & 3.969 \cdot 10^{-5} & 0 \\ 0 & 0 & 0 & 0 & 3.41 \cdot 10^{-6} \end{pmatrix}$$

In this case the σ_{12} element of the matrix is no zero because the initial beam has a waist only on y but not on x (Fig.3).

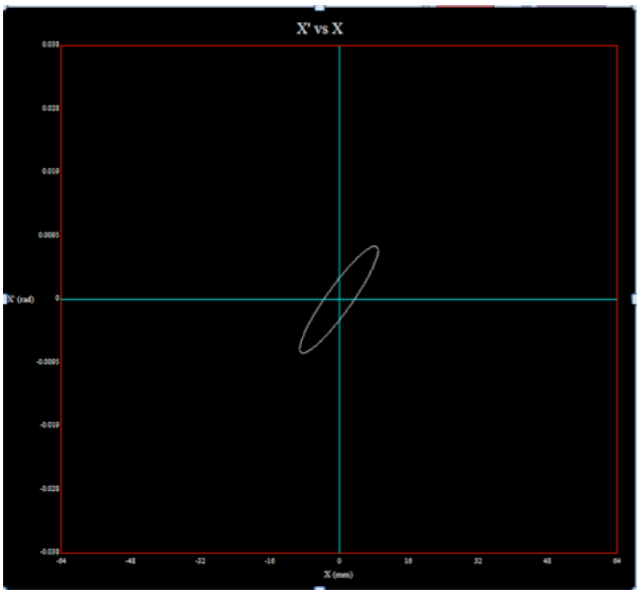

Figure 3: X vs X' plot of the initial beam.

Since

$$r_{12} = \frac{\sigma_{12}}{\sqrt{\sigma_{11}\sigma_{22}}}$$

where r_{12} describes the inclination of the ellipse and is equal 0.92, we obtain that σ_{12} is equal to 0.06624.
The following step is the setting of the drifts length and the quadrupole parameters.
The beam envelope, in the horizontal plane and in the vertical plane, obtained running the simulation for both the configuration are reported in fig. 4 and fig.5.

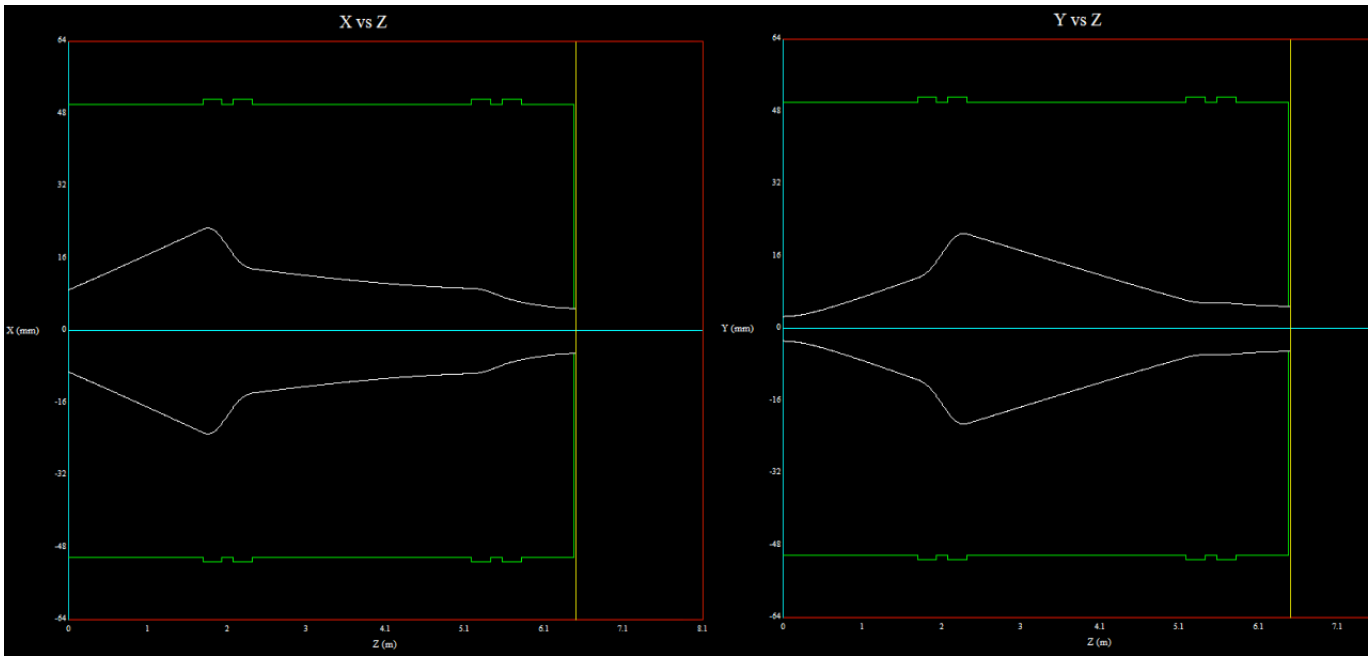

Figure 4: Beam envelope (simulated with *Beamline Simulator Software*) in the horizontal plane and in the vertical plane for the circular beam spot diameter of 10 mm.

The maximum beam size calculated with Transport for both tunes is 35 mm, while we find that the beam envelope maximum size is less the 12 mm on the vertical plane and less then 23 mm on the horizontal plane. This is probably due to the differences in the programs used for the simulation and also the fact that in Transport is was considered the 99% of the beam inside the envelope while we consider the 95%.
Nevertheless for both configurations, we find a good agreement between our simulations and Trnsport results as it is possible to note from the data tables 3 and 4.

Table 3: Radius along x and y of the beam spot on target of 10 mm from IBA results and from our simulation.

	Transport results (mm)	Our results (mm)
R_x	5.0	5.0002
R_y	5.0	4.9980

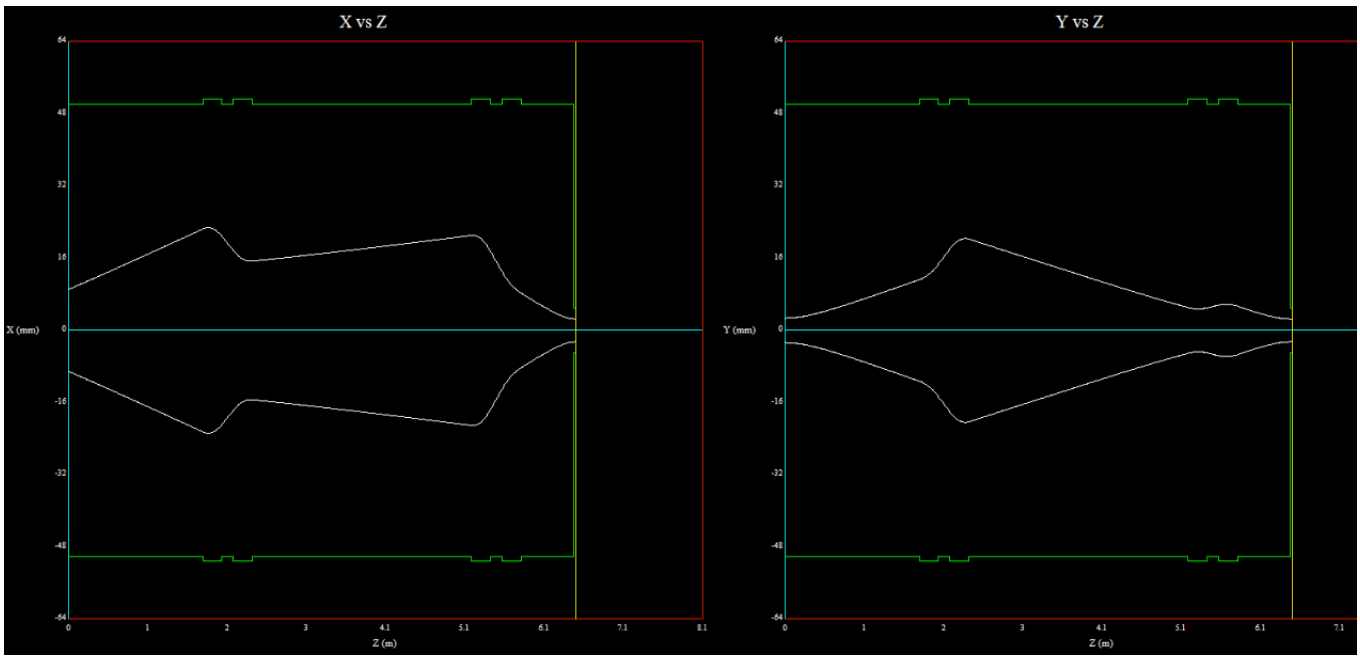

Figure 5: Beam envelope (simulated with *Beamline Simulator Software*) in the horizontal plane and in the vertical plane for the circular beam spot diameter of 5 mm.

Table 4: Radius along x and y of the beam spot on target of 5 mm from IBA results and from our simulation.

	Transport results (mm)	Our results (mm)
R_x	2.5	2.5039
R_y	2.5	2.5008

4 Robustness

In order to check the robustness of the tunes, changes of the beam envelopment have been studied as a function of the beam line parameters such as quadrupole fields, quadrupole doublet' position along the line and initial misalignment of the beam.

4.1 Shifts of quadrupole doublets

We simulated the effects of a possible wrong positioning of the quadrupole along the beam line.

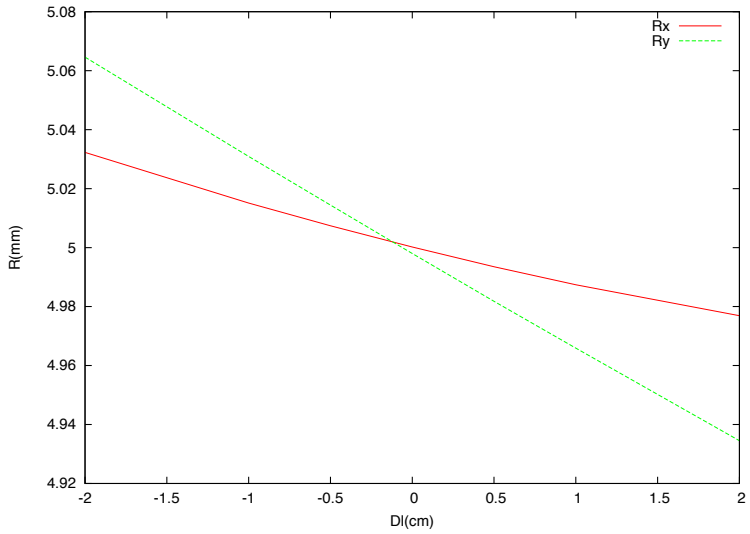

Figure 6: Dependence of R_x (red plot) and R_y (green plot) from a ΔL shift of the first quadrupole doublet.

In figure 8 is plotted in red the x radius (R_x) and in green y radius (R_y) of the beam spot at target as a function of the shift ΔL of the first doublet; the same plot for the second doublet is reported in Fig.9.
The beam envelope on the xy plane shows a good stability; along both the axis the changes in the spot radius are less than 0.05 mm for a maximum shift ΔL of 2 cm.
According to the position of the magnets in the order of a few mm, a good robustness is guaranteed. As the precision of the mechanical mounting is 1 mm, no problems are to be expected.

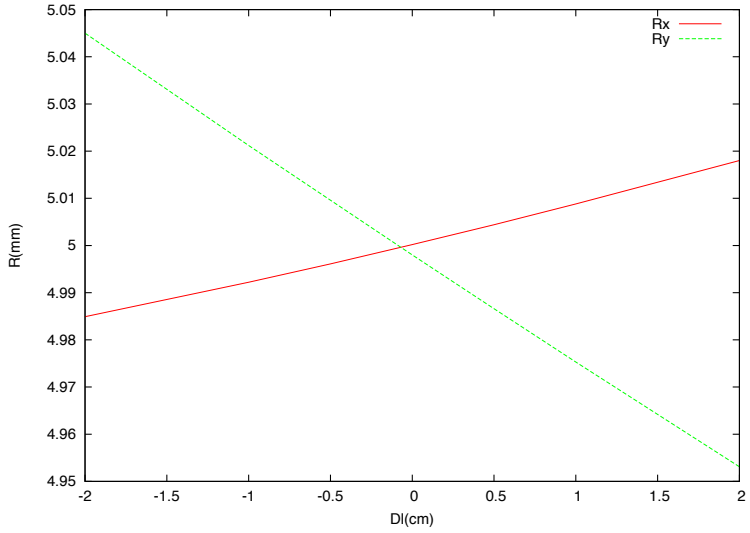

Figure 7: Dependence of R_x (red plot) and R_y (green plot) from a ΔL shift of the second quadrupole doublet.

4.2 Variations of the quadrupoles magnetic field

We've changed the setting of the magnetic fields of each quadrupole individually till a maximum offset of 40 G.
The plot related to the horizontal focusing quadrupole of the first doublet is reported in Fig.8 while the plot for the vertical focusing one is in Fig.9.
The results of the calculations show, that changes in the vertical magnetic field have a bigger influence than changes in the horizontal field.
Still, the maximum shift of the beam spot is less than 1 mm both along x (red plot) and y (green plot).

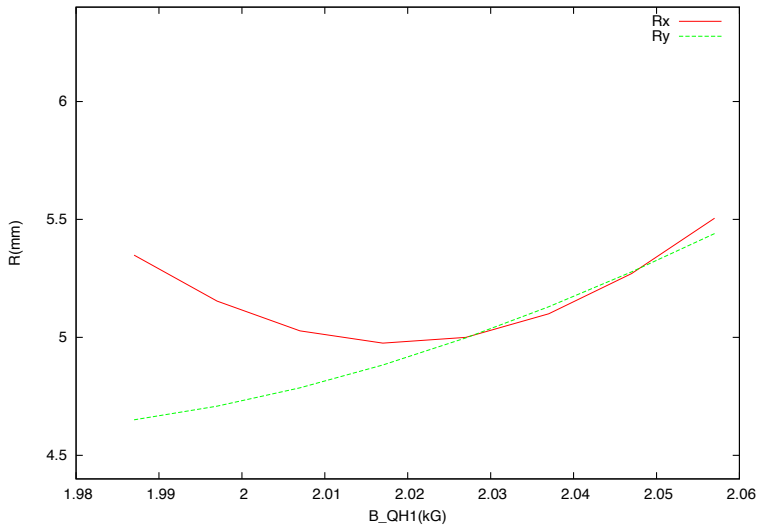

Figure 8: R_x (red plot) and R_y (green plot) as a function of the magnetic field of the first horizontal focusing quadrupole (HQ1).

In Fig. 10 and 11 is plotted in red the x and in green the y beam spot radius as a function of the magnetic field of the second doublet quadrupoles.
Due to the shorter flight-length after the second magnet, the effects of magnetic field variations are much smaller than for the first magnet, the variations introduce only an offset of 0.3 mm for the beam spot.
In table 5 the maximum variation for the beam spot due to each of the quadrupoles are reported.

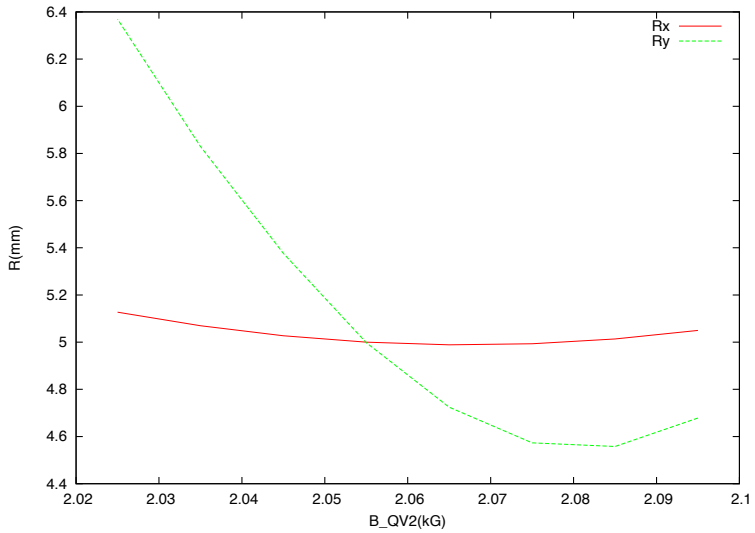

Figure 9: R_x (red) and R_y (green) as a function of the magnetic field of the first vertical focusing quadrupole (VQ2).

Table 5: Maximum radius variation along x and y of the beam spot on target of 10 mm at the maximum offset of the magnetic field of the four quadrupole.

Quadrupole	ΔR_x (mm)	ΔR_y (mm)
HQ1	0.51	0.44
VQ2	0.13	1.37
HQ3	0.26	0.18
VQ4	0.15	0.12

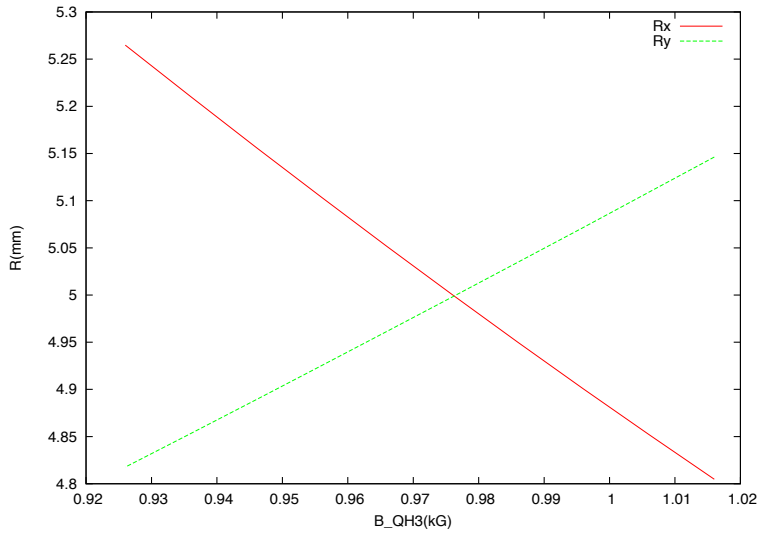

Figure 10: R_x (red plot) and R_y (green plot) as a function of the magnetic field of the second horizontal focusing quadrupole (HQ3).

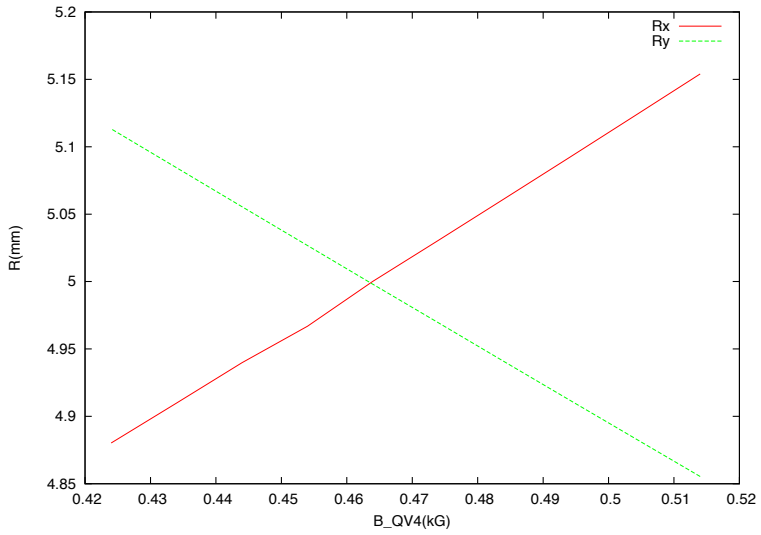

Figure 11: R_x (red plot) and R_y (green plot) as a function of the magnetic field of the second vertical focusing quadrupole (VQ4).

4.3 Variation of the emittance

To crosscheck the effects of the initial emittance, which is given only as an approximation by IBA, we investigated how changing the emittance parameters affects the beam spot at the target.
In Fig.12 we have plotted the dependence of R_x from the initial σ_{11} value and in Fig.13 from the initial σ_{22} value, while in Fig.14 is reported the dependence of R_x from the initial σ_{33} value and in Fig.15 from the initial σ_{44} value.
If the real emittance of our cyclotron is smaller than the IBA 30/30, we will have a smaller beam spot finally.

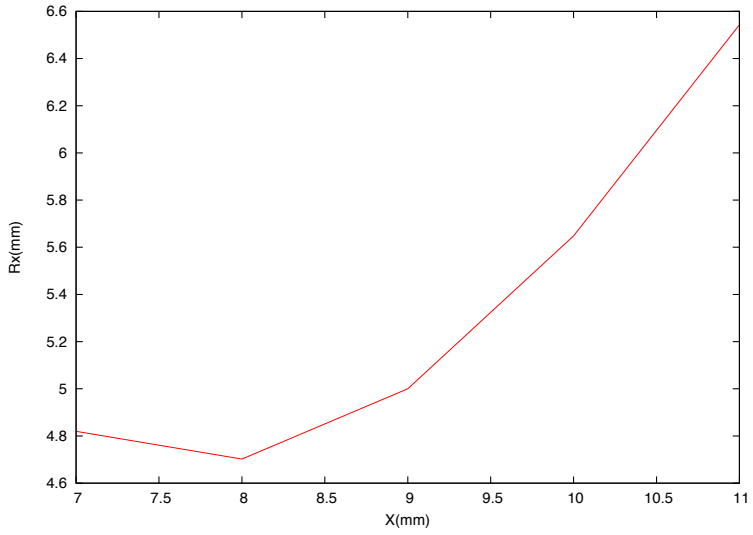

Figure 12: x radius of the spot beam at the target as a function of σ_{11} (x).

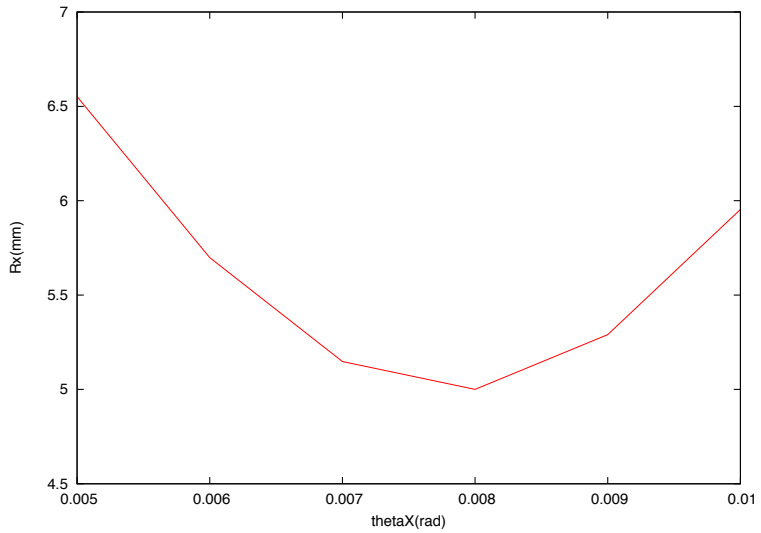

Figure 13: x radius of the spot beam at the target as a function of σ_{22} (x').

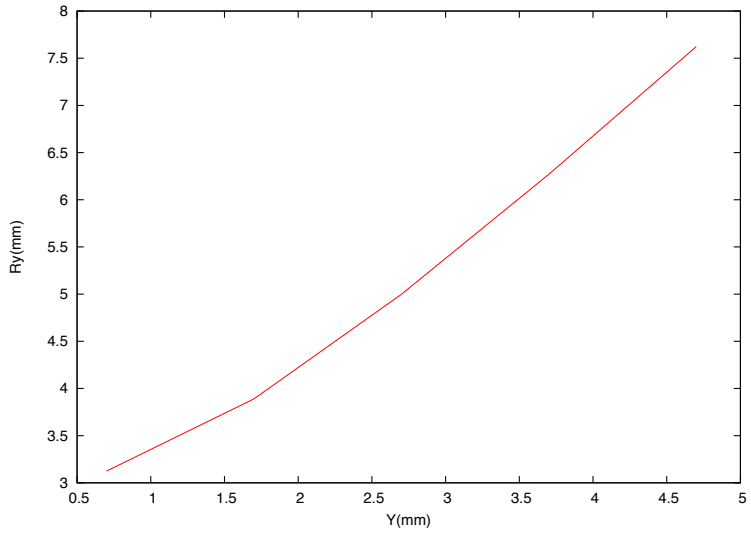

Figure 14: y radius of the spot beam at the target as a function of σ_{33} (y).

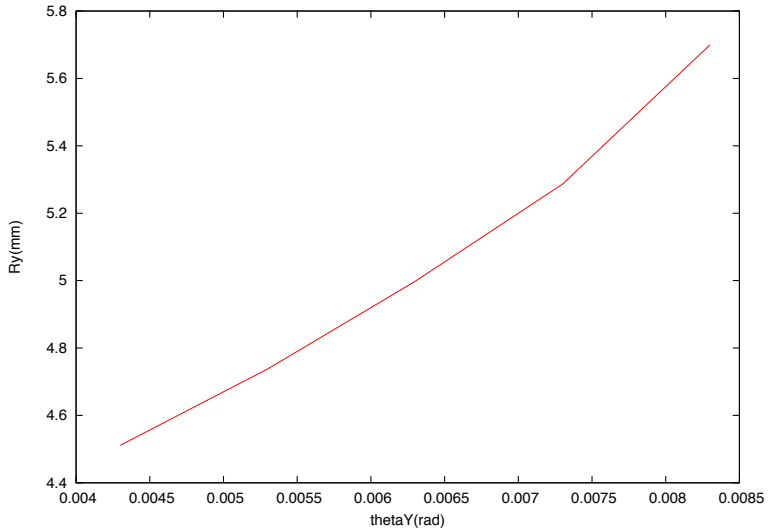

Figure 15: y radius of the spot beam at the target as a function of σ_{44} (y').

4.4 Simulation of an initial misalignment of the beam

An inaccurate positioning of carbon foil stripper can lead to a shift of the beam in the horizontal plane and consequently to a loss of part of the beam.

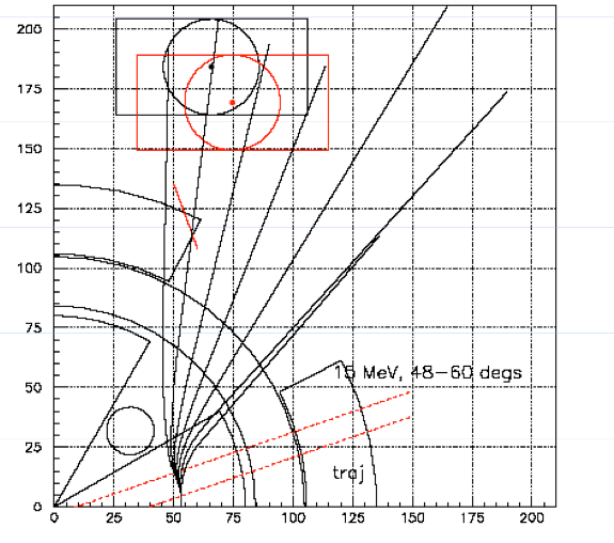

Figure 16: Extraction through carbon foil stripper.

The program allows the simulation of this effect through the 'Beam Perturbation' element introduced just after the beam source.
This element permits to reproduce a shift of the beam on x and also a divergence of the envelope. In Fig.17 is shown the fraction of beam hitting the target as function of the beam shift along x; when the deviation become more then 6 mm most of the beam is lost.
While in Fig.18 is shown the decreasing of the incident beam on the target when a perturbation defocuses the beam in the x direction just after the source.

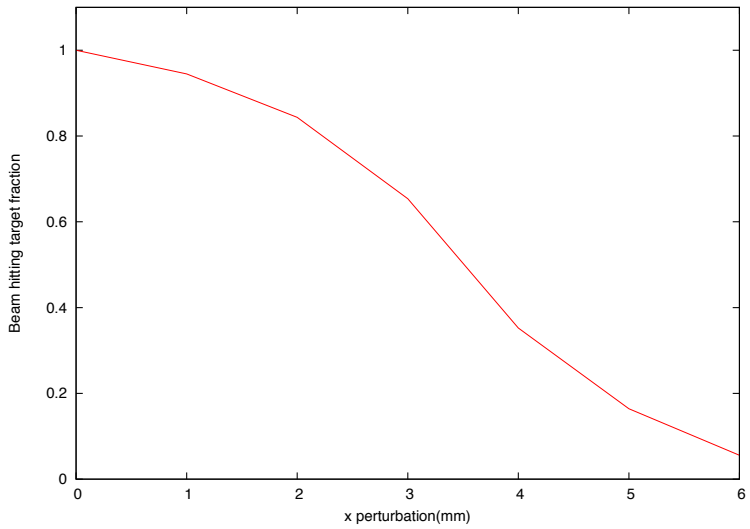

Figure 17: Incident beam behavior at the variation of the x shift.

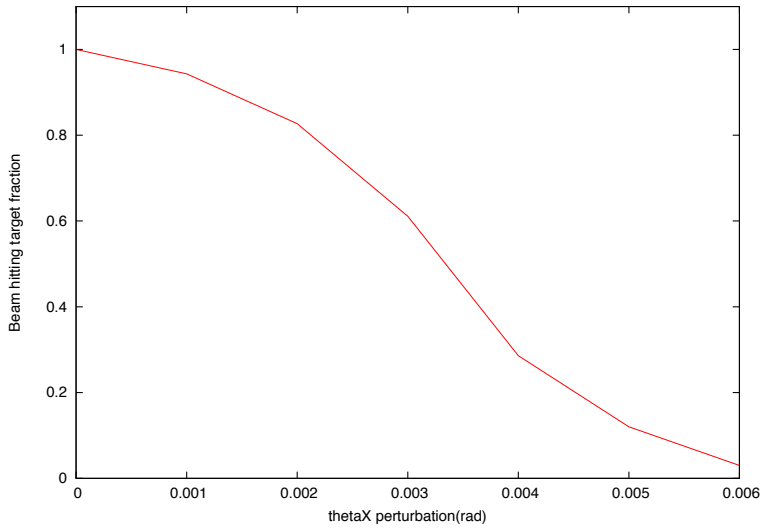

Figure 18: Incident beam behavior at the variation of x' parameter (introduction of a defocusing effect along x).

4.5 Low currents

The C18/18 cyclotron is guaranteed for a minimum current of 10 μA up to a maximum current of 150 μA.
We're interested to reduce the current to approximately 1 nA for detector testing and radiobiology studies.
To decrease the current along the simulated beam line two collimator with square apertures and 2 *cm* length have been introduced; the first collimator (collimator 1 or also called before *drum collimator*) is settled 678 *mm* before the first quadrupole doublet and the second (collimator 2) is at the end of the line just before the target.
In Fig.19 is plotted the decreasing of particles hitting the target when just the collimator 1 is introduce along the beam line (red plot) and then when there is only the collimator 2 at the target (green plot).
In Fig.20, the effect of both collimators is shown by varying the opening gap of collimator 1 (one color line for each aperture size); the final beam current is shown in dependance of the opening gap of collimator 2; from these in evident that to reduce the current by $\frac{1}{1000}$ both the collimator must have an aperture size of 1 *mm*.
Variations of the size of the collimator, from 2 *cm* up to 10 *cm* show no changes in the final beam current.
From these simulation seems that the fraction of beam hitting the target depends only on aperture size of the collimators.

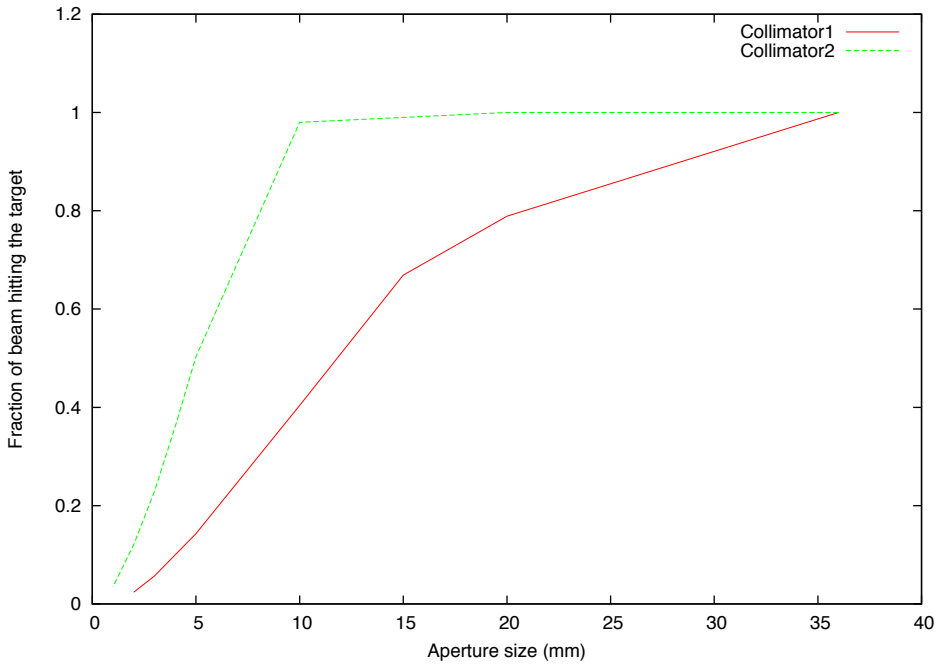

Figure 19: Fraction of beam hitting the target as function of aperture size of collimator 1 (at the target) in red and of aperture size of collimator 2 (drum collimator) in green.

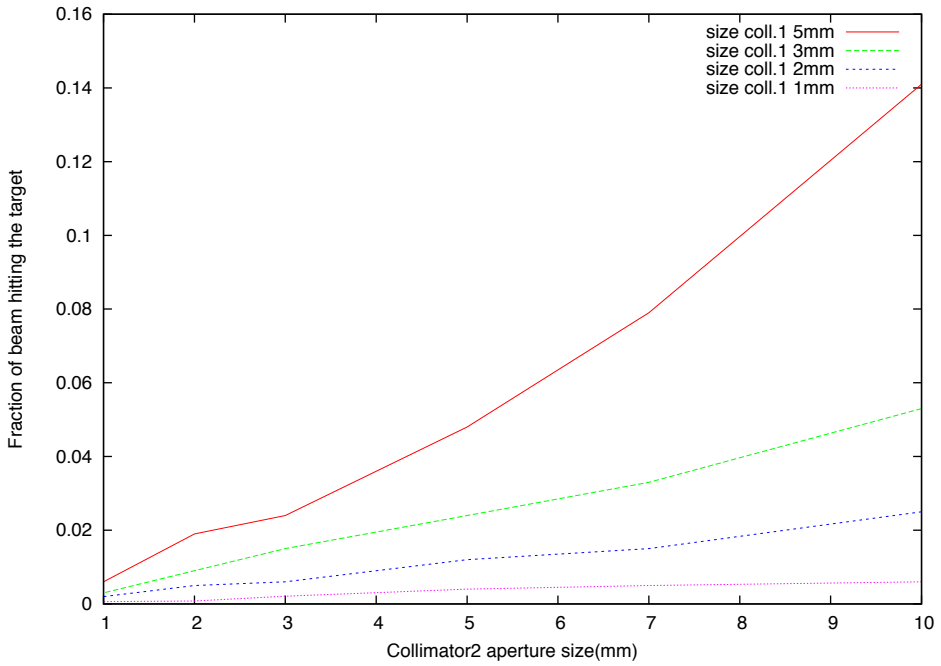

Figure 20: Fraction of beam hitting the target as function of aperture size of collimator 2 when the collimator 1 has an aperture size of 5 mm (red), 3 mm (green), 2 mm (blue) and 1 mm (pink).

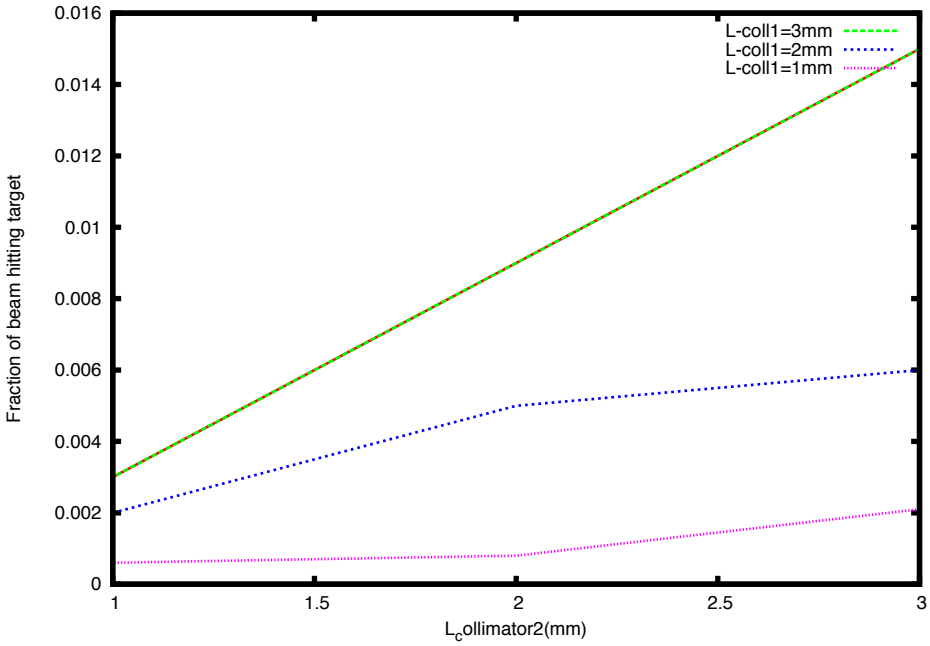

Figure 21: Fraction of beam hitting the target as function of aperture size of collimator 2 in the range from 1 to 3 mm when the collimator 1 has an aperture size of 5 mm (red), 3 mm (green), 2 mm (blue) and 1 mm (pink).